FACULTY OF MECHANICAL ENGINEERING CTU IN PRAGUE

DEPARTMENT OF ENVIRONMENTAL ENGINEERING

UNIVERSITY CENTRE FOR ENERGY EFFICIENT BUILDINGS CTU IN PRAGUE

TITLE

TRNSYS TYPE 206

MODEL OF GLAZED SOLAR AIR COLLECTOR BASED ON DETAILED CONSTRUCTION PARAMETERS AND ENERGY BALANCE

AUTHORS

Viacheslav Shemelin

Tomáš Matuška

Bořivoj Šourek

PAGES 19

ANNEXES 1

DATE October 2017

Contents

1. Introduction

The presented Type 206 is a detailed mathematical model developed for thermal performance simulation of four different solar air collector designs. The considered designs are shown in Fig. 1: Design 1 – Single channel design with single air flow between transparent cover and bottom absorber plate; Design 2 – Double channel design with single air flow between absorber and bottom plate; Design 3 (not availibly yet) – Double channel design with double air flows between transparent cover and absorber plate and between absorber and bottom plate; Design 4 (not availibly yet) – Double channel design with double-pass air flow.

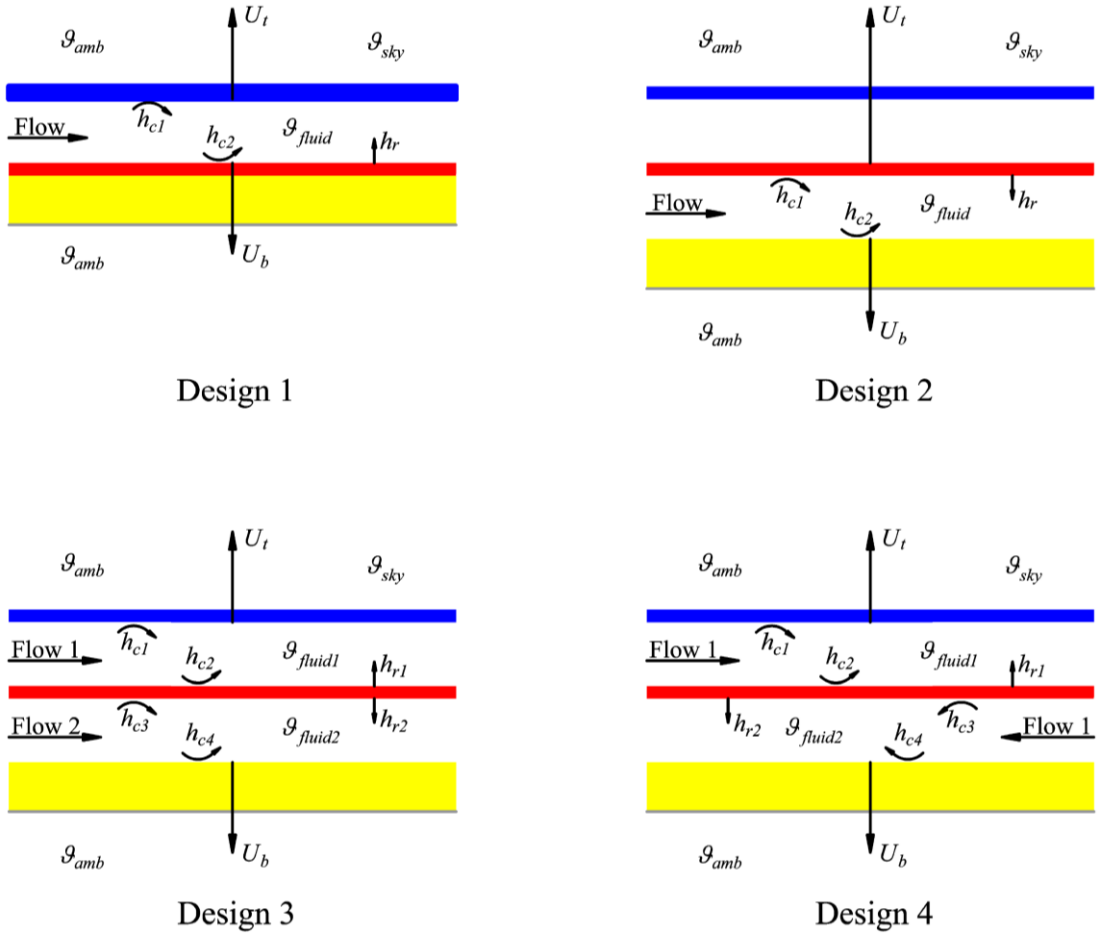

Fig. 1 – The considered solar air collector desings

The solar air collector can be specified by a number of detailed parameters, optical properties of the transparent cover and the absorber and thermophysical properties of main components of the solar collector. Moreover, the transparent cover (glazing, plastic or another transparent insulation structure) and the back thermal insulation are defined by temperature dependent thermal conductance.

The implementation of the model in TRNSYS environment offers the parametric analysis for different construction alternatives for annual solar collector performance in the given solar system application. There is also a possibility to change mathematical models describing the fundamental heat transfer phenomena (natural convection, wind convection, forced convection, etc.) and perform sensitivity analysis for selection of the models.

2. Parameter-List

Nr.	*short*	*explanation*	*unit*	*range*
1	M_1	Solar air collector Design	[-]	[1;4]
2	A	Collector width	*m*	[0;inf]
3	B	Collector height	*m*	[0;inf]
4	C	Collector length	*m*	[0;inf]
5	A_{abs}	Absorber area	m^2	[0;inf]
6	a_f	Front air channel width	*m*	[0;inf]
7	b_f	Front air channel height	*m*	[0;inf]
8	c_f	Front air channel length	*m*	[0;inf]
9	a_b	Back air channel width	*m*	[0;inf]
10	b_b	Back air channel height	*m*	[0;inf]
11	c_b	Back air channel length	*m*	[0;inf]
12	ε_{c1}	External surface emissivity of cover (f_1)	[-]	[0;1]
13	ε_{c2}	I surface emissivity of cover (f_2)	[-]	[0;1]
14	$\varepsilon_{abs,f}$	Front surface emissivity of absorber	[-]	[0;1]
15	$\varepsilon_{abs,b}$	Back surface emissivity of absorber	[-]	[0;1]
16	ε_{ins}	Internal surface emissivity of insulation (b_1)	[-]	[0;1]
17	ε_{fs}	External surface emissivity of frame (b_2)	[-]	[0;1]
18	ε_{as}	Emissivity of adjacent surfaces	[-]	[0;1]
19	τ_n	Solar transmittance of the collector cover	[-]	[0;1]
20	α_{abs}	Solar absorptance of the absorber	[-]	[0;1]
21	b_0	1st-order incidence angle modifier (IAM)	[-]	[0;1]
22	b_1	2nd-order incidence angle modifier (IAM)	[-]	[-1;1]
23	h_{cov0}	Thermal conductance of cover 0	$W/m^2.K$	[0;inf]
24	h_{cov1}	Thermal conductance of cover 1	$W/m^2.K^2$	[-inf;inf]
25	h_{cov2}	Thermal conductance of cover 2	$W/m^2.K^3$	[-inf;inf]
26	h_{ins0}	Thermal conductance of back insulation 0	$W/m^2.K$	[0;inf]
27	h_{ins1}	Thermal conductance of back insulation 1	$W/m^2.K^2$	[-inf;inf]
28	h_{ins2}	Thermal conductance of back insulation 2	$W/m^2.K^3$	[-inf;inf]
29	M_2	Wind convection model Mode	[-]	[1;4]
30	M_3	Natural convection model Mode	[-]	[1;6]
31	M_4	Forced convection model Mode	[-]	[1;7]
32	M_5	Calculation Mode	[-]	[1;2]

3. Input-List

Nr.	*short*	*explanation*	*unit*	*range*
1	t_{in}	Inlet air temperature	*°C*	[-inf;+inf]
2	$\dot{M}$	Inlet air flowrate	*kg/h*	[0;inf]
3	t_{amb}	Ambient temperature	*°C*	[-inf;+inf]
4	t_{sky}	Sky temperature	*°C*	[-inf;+inf]
5	I_{beam}	Beam radiation for collector surface	$kJ/h.m^2$	[0;inf]
6	I_{sky}	Sky diffuse radiation for collector surface	$kJ/h.m^2$	[0;inf]
7	I_{gnd}	Ground reflected diffuse radiation for collector surface	$kJ/h.m^2$	[0;inf]
8	θ	Incidence angle	*deg*	[0;+inf]
9	φ	Collector slope	*deg*	[0;90]
10	w	Wind velocity	*m/s*	[0;+inf]

4. Output-List

Nr.	*short*	*explanation*	*unit*	*range*
1	t_{out}	Outlet air temperature	*°C*	[-inf;+inf]
2	$\dot{M}$	Outlet air flowrate	*kg/h*	[0;inf]
3	Φ_{out}	Useful energy gain of collector	*kJ/h*	[-inf;+inf]
4	η	Collector thermal efficiency	[-]	[0;1]
5	t_{abs}	Absorber mean temperature	*°C*	[-inf;+inf]

5. Units conversion

In the table above, there are several non-SI units. The presented Type 206 computes in the SI units, which are more convenient for calculations. Therefore all non-SI units have to be converted into SI units. The conversion of some non-SI units into SI units is given in Tab. 1.

Tab. 1 – Conversation of non-SI units

Dimension	Non-SI unit	Equivalence in SI-units
Temperature	t [°C]	$\vartheta = t + 273.15$ [K]
Mass flow	$\dot{M}$ [kg/h]	$\dot{m} = \frac{\dot{M}}{3600}$ [kg/s]
Energy flux	I [kJ/h.m^2]	$G = \frac{I}{3.6}$ [W/m^2]
Power	Φ_{out} [kJ/h]	$\dot{Q}_u = \frac{\Phi_{out}}{3.6}$ [W]

6. Basic equations

The core of the Type 206 is a mathematical model for solar air collector solving one-dimensional heat transfer balances. The thermal networks for four designs of solar collectors considered are shown in Fig. 2.

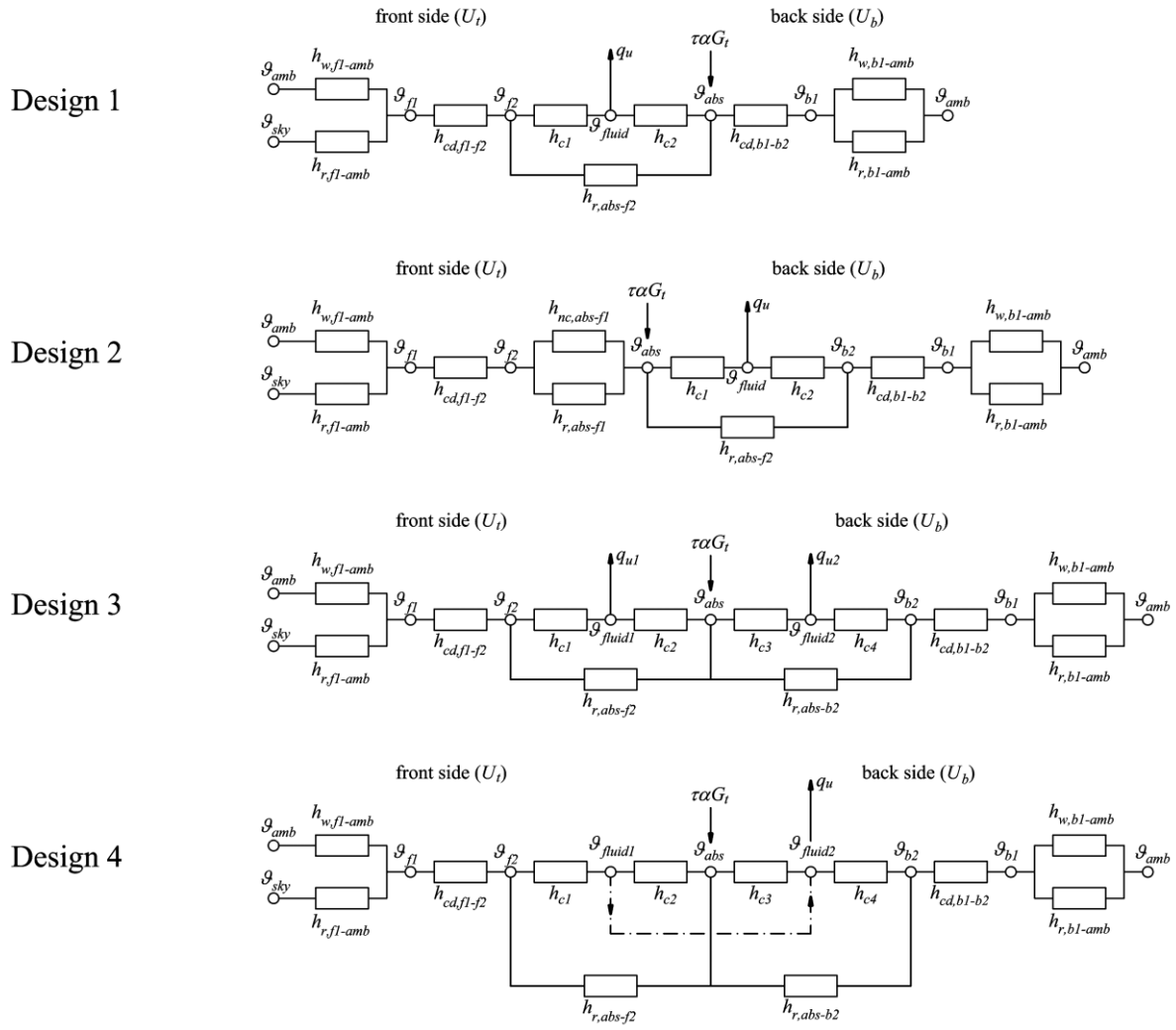

Fig. 2 – Thermal network for solar air collectors

To illustrate the procedure for deriving of usable heat gain Q_u, efficiency with respect to reference collector area (gross area A_G), and output heat transfer fluid temperature t_{out}, we derive equations for the most common design of air collector – Design 2 in Fig. 1. The equations for other designs are derived in a similar manner.

Because heat transfer coefficients are temperature dependent, a set of mean temperatures is approximated which allows the heat transfer coefficients to be evaluated as a first guess:

$$\vartheta_{fluid} = \vartheta_{in} + 20 \qquad [\mathrm{K}] \qquad (1)$$

$$\vartheta_{abs} = \vartheta_{in} + 10 \qquad [\mathrm{K}] \qquad (2)$$

Then the surface temperatures are estimated from temperature difference between absorber and ambient environment uniformly as follows:

$$\vartheta_{f1} = \vartheta_{b1} = \vartheta_{abs} - \frac{\vartheta_{abs} - \vartheta_{amb}}{3} \qquad [\mathrm{K}] \qquad (3)$$

$$\vartheta_{f2} = \vartheta_{b2} = \vartheta_{amb} + \frac{\vartheta_{abs} - \vartheta_{amb}}{3} \qquad [\mathrm{K}] \qquad (4)$$

After that heat transfer coefficients can be calculated and collector heat loss coefficients U_t (top) and U_b (back) can be obtained. Since these coefficients have been calculated for incorrect temperatures, next iteration step follows. From heat transfer coefficients and heat flows through front and back side of collector the temperature distribution can be obtained by reverse calculation process. To evaluate the new mean temperatures two different calculation Modes are used. Mode 1 is based on the Hottel-Whiller-Bliss [1–4] general equation for solar collector performance. Mode 2 uses the heat balances equations for each temperature level and matrix inversion method. The newly-calculated mean temperatures are then compared with the initially-guessed temperatures. The iterative process is repeated until all consecutive results of mean temperatures differ by less than 0.01 K. The scheme of iteration loop is outlined in Fig. 3.

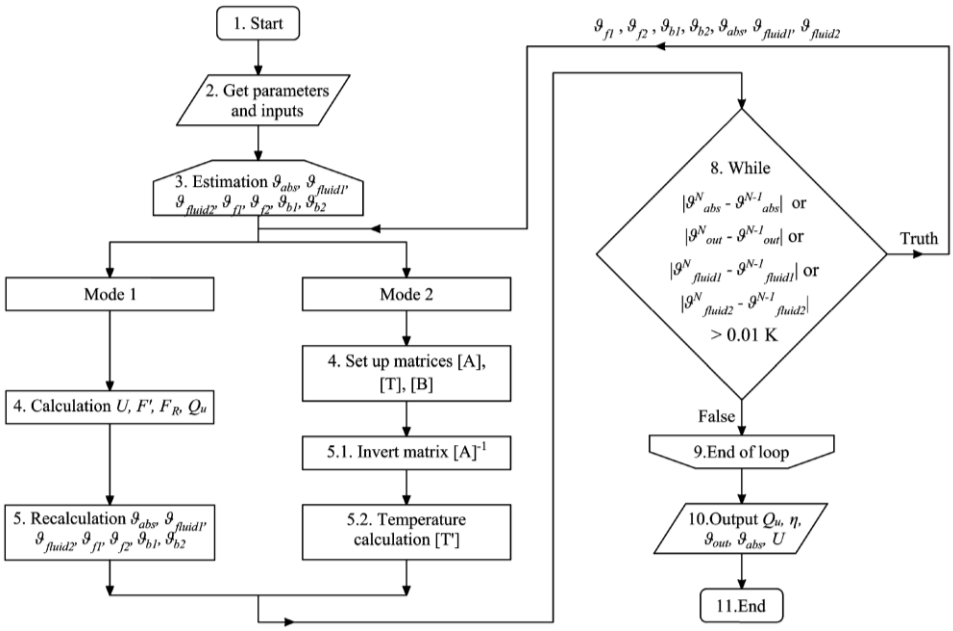

Fig. 3 – Flow chart of iteration loop

6.1. Radiation heat transfer between top surface and sky

To describe the radiation heat transfer between top surface and sky, the sky area is considered as a black body of equivalent temperature ϑ_{sky}. Equivalent sky temperature ϑ_{sky} is introduced due to fact that sky temperature is not uniform and constant and atmosphere radiates only in certain wavelengths ranges in reality.

Radiation heat transfer coefficient is given by

$$h_{r,f1-amb} = \varepsilon_{f1}\sigma \frac{\vartheta_{f1}^4 - \vartheta_{sky}^4}{\vartheta_{f1} - \vartheta_{amb}} \quad [\mathrm{W/m^2.K}] \tag{5}$$

where

σ is Stefan-Boltzmann constant, $\sigma = 5.67\times10^{-8}$ W/m^2.K^4.

6.2. Wind convection heat transfer from top and bottom surfaces to ambient

Heat transfer by convection from exterior surface of transparent cover or back side to ambient environment under realistic conditions (mixed natural and forced wind convection) is quite problematic. A large number of relationships and correlations derived from experiments, more or less reproducing the boundary conditions of solar collector installation, can be found in literature (see Tab. 2).

Tab. 2 – Wind convection correlations

M_2	Author	Equation	Range
1	McAdams [5]	$h_{w,s-amb} = 5.7 + 3.8w$ $h_{w,s-amb} = 6.47w^{0.78}$	for $w < 5$ m/s for $w > 5$ m/s
2	Watmuff [6]	$h_{w,s-amb} = 2.3 + 3.0w$	$0 < w < 7$ m/s
3	Test [7,8]	$h_{w,s-amb} = 8.55 + 2.56w$	$0 < w < 5$ m/s
4	Kumar [9]	$h_{w,s-amb} = 10.03 + 4.687w$	$0 < w < 4$ m/s

6.3. Conduction through transparent cover and insulation material

For a single cover glazing the conductance can be considered as a constant and calculated as

$$h_{cd,f1-f2} = \frac{\lambda}{d_{f1-f2}} \quad [\mathrm{W/m^2.K}] \tag{6}$$

where

λ thermal conductivity of cover, W/m.K;

$d_{f1\text{-}f2}$ thickness of cover, m.

In the case of transparent insulation material or in the case of back insulation, thermal conductance of the structure could be determined as a function of mean temperature $\vartheta_{s1\text{-}s2}$

$$h_{cd,s1-s2} = f(\vartheta_{s1-s2}) = h_{cov0} + h_{cov1}\vartheta_{s1-s2} + h_{cov2}\vartheta^2_{s1-s2} \quad [\mathrm{W/m^2.K}] \tag{7}$$

6.4. Natural convection in closed gas layer between absorber and transparent cover

Heat transfer by natural convection in the closed gas layer between absorber and transparent cover is characterized by Nusselt number Nu related to characteristic dimension of the layer, the thickness b_f. Geometric parameters of the gas layer and heat flow direction (upward) are outlined in Fig. 4.

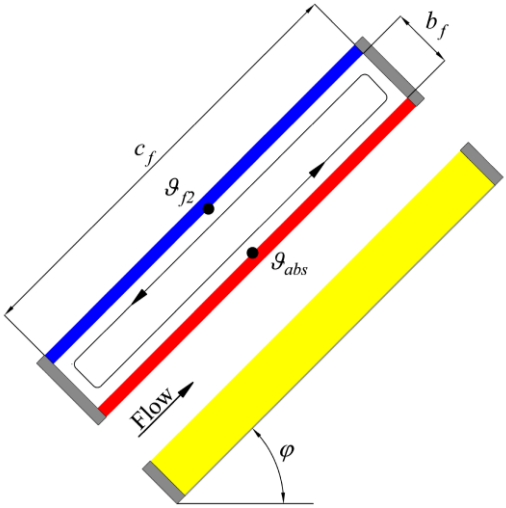

Fig. 4 – Natural convection in closed gas layer (Design 2)

Natural convection heat transfer coefficient for closed inclined layer between absorber and cover glazing can be obtained from

$$h_{nc} = \frac{\mathrm{Nu}\lambda_g}{b_f} \quad [\mathrm{W/m^2.K}] \tag{8}$$

where

λ_g is thermal conductivity of still gas for mean temperature $\vartheta_{abs\text{-}f1}$ in the gas layer, W/m.K.

Nusselt number for natural convection is dependent on Rayleigh number Ra, i.e. product of Grashof number Gr and Prandtl number Pr.

$$\mathrm{Ra} = \mathrm{Gr}\,\mathrm{Pr} \quad [-] \tag{9}$$

Prandtl number can be obtained from the properties of used gas at mean temperature of the layer $\vartheta_{abs\text{-}f1}$ as given

$$\mathrm{Pr} = \frac{\nu\rho c}{\lambda} \quad [-] \tag{10}$$

where

ν is kinematic viscosity of gas, m^2/s;

ρ density of gas, kg/m^3;

c specific thermal capacity of gas, J/kg.K.

Grashof number Gr_b is given by

$$\mathrm{Gr} = \frac{\beta g b_{f1}^3 \Delta\vartheta}{\nu^2} = \frac{1}{\vartheta_{abs-f1}} \frac{g b_{f1}^3 \left(\vartheta_{abs} - \vartheta_{f1}\right)}{\nu^2} \quad [-] \tag{11}$$

where

β is volumetric thermal expansion coefficient, 1/K;

g gravity acceleration, m/s^2.

Number of published experiments and derived correlations has been found for natural convection heat transfer in sloped enclosure (Tab. 3).

Tab. 3 – Selected correlations for natural convection in the sloped closed gas layer

<table>
<tr><th rowspan="2">M_3</th><th rowspan="2">Author</th><th rowspan="2">Equation</th><th colspan="3">Range</th></tr>
<tr><th>Ra</th><th>φ</th><th>c_f/b_f</th></tr>
<tr><td>1</td><td>Hollands [10]</td><td>$\mathrm{Nu}=1+1.44\left[1-\frac{1708}{\mathrm{Ra}\cos\varphi}\right]^{+}\left(1-\frac{(\sin\varphi)^{1.6}1708}{\mathrm{Ra}\cos\varphi}\right)+\left[\left(\frac{\mathrm{Ra}\cos\varphi}{5830}\right)^{1/3}-1\right]^{+}$</td><td>0< Ra<$10^5$</td><td>0°-60°</td><td>cca 48</td></tr>
<tr><td>2</td><td>Buchberg [11]</td><td>$\mathrm{Nu}_b=1+1.44\left[1-\frac{1708}{\mathrm{Ra}\cos\varphi}\right]^{+}$
$\mathrm{Nu}=0.229(\mathrm{Ra}\cos\varphi)^{0.252}$
$\mathrm{Nu}=0.157(\mathrm{Ra}\cos\varphi)^{0.285}$</td><td>1708< Racos$\varphi$<$10^5$
5900< Racosφ<9.2x10^4
9.2x10^4< Racosφ<10^6</td><td>0°-60°</td><td></td></tr>
<tr><td>3</td><td>Randal [12]</td><td>$\mathrm{Nu}=0.118\left[\mathrm{Ra}\cos^2(\varphi-45)\right]^{0.29}$</td><td>2.8x$10^3$< Racos$\varphi$<2.2x$10^5$</td><td>45°-90°</td><td>9-36</td></tr>
<tr><td>4</td><td>Schinkel [13]</td><td>$\mathrm{Nu}=a(\varphi)\mathrm{Ra}^{1/3}$
<table>
<tr><th>φ</th><th>$a(\varphi)$</th></tr>
<tr><td>0°</td><td>0.080</td></tr>
<tr><td>10°</td><td>0.079</td></tr>
<tr><td>20°</td><td>0.075</td></tr>
<tr><td>30°</td><td>0.074</td></tr>
<tr><td>40°</td><td>0.074</td></tr>
</table>
<table>
<tr><th>φ</th><th>$a(\varphi)$</th></tr>
<tr><td>50°</td><td>0.074</td></tr>
<tr><td>60°</td><td>0.072</td></tr>
<tr><td>70°</td><td>0.069</td></tr>
<tr><td>80°</td><td>0.068</td></tr>
<tr><td>90°</td><td>0.062</td></tr>
</table></td><td>10^5< Racosφ<4x10^6</td><td>0°-90°</td><td>6-27</td></tr>
<tr><td>5</td><td>Niemann [14]</td><td>$\mathrm{Nu}=1+\frac{m(\mathrm{Ra})^c}{\mathrm{Ra}+n}$
<table>
<tr><th>φ</th><th>m</th><th>n</th><th>c</th></tr>
<tr><td>0°</td><td>0.0700</td><td>0.32x10^4</td><td>1.333</td></tr>
<tr><td>45°</td><td>0.0430</td><td>0.41x10^4</td><td>1.360</td></tr>
<tr><td>90°</td><td>0.0236</td><td>1.01x10^4</td><td>1.393</td></tr>
</table></td><td>10^2< Ra<10^8</td><td></td><td></td></tr>
<tr><td>6</td><td>Matuska [15]</td><td>$\mathrm{Nu}=\left(0.1464-2.602\times10^{-4}\varphi-2.046\times10^{-6}\varphi^2\right)\mathrm{Ra}^{0.29}$</td><td colspan="3">integral correlation (see [5])</td></tr>
<tr><td colspan="6">superscript + indicates that content of brackets is considered only for positive values, for negative values the content is equal to 0.</td></tr>
</table>

6.5. Radiation heat transfer between parallel plates

Radiation heat transfer coefficient between absorber and interior surface of transparent cover or between absorber and insulation can be obtained from

$$h_{r,abs-s}=\frac{\sigma}{\frac{1}{\varepsilon_{abs}}+\frac{1}{\varepsilon_s}-1}\frac{\vartheta_{abs}^4-\vartheta_s^4}{\vartheta_{abs}-\vartheta_s}\qquad [\mathrm{W/m^2.K}] \tag{12}$$

6.6. Forced convection between parallel plates

To handle forced convection between two parallel plates, both correlations developed especially for parallel plates and many correlations developed for circular tubes may be applied. In both cases, an effective diameter should be used as the characteristic length. It is termed the hydraulic diameter and it is defined as

$$D_h=\frac{4A}{P}\qquad [\mathrm{m}] \tag{13}$$

where

A is the flow cross-sectional area, $\mathrm{m^2}$;

P the perimeter wetted by fluid, m.

Then forced convection heat transfer coefficient is determined from Nusselt number

$$h_c = \mathrm{Nu}_D \frac{\lambda_f}{D_h} \ [\mathrm{W/m^2.K}] \qquad (14)$$

where

λ_f is thermal conductivity of heat transfer fluid, W/m.K;

In the presented Type 206, the coefficients for both upper and lower surfaces of each channel are assumed equal, $h_{c1} = h_{c2}$ and $h_{c3} = h_{c4}$.

6.6.1. Turbulent flow region (Re > 10000)

Turbulent forced convection heat transfer is widely described. Tab. 4 shows correlations for Nusselt number for turbulent forced convection heat transfer found in the literature.

Tab. 4 – Selected correlations for turbulent flow region

M_4	Author	Equation	Comment
1	Kays and Crawford [16]	$\mathrm{Nu}_D = 0.0158\,\mathrm{Re}_D^{0.8}$	developed for solar air collectors, Re > 3000
2	Tan and Charters [17]	$\mathrm{Nu}_D = 0.018\,\mathrm{Re}_D^{0.8}\,\mathrm{Pr}^{0.4}$	developed for solar air collectors, 9500 < Re < 22000
3	Nusselt [18]	$\mathrm{Nu}_D = 0.036\,\mathrm{Re}_D^{0.8}\,\mathrm{Pr}^{1/3}(D_h/L)^{0.055}$	developed for circular tube, 10 < *L*/*D* < 400
4	Sieder and Tate [19]	$\mathrm{Nu}_D = 0.027\,\mathrm{Re}_D^{0.8}\,\mathrm{Pr}^{1/3}(\mu/\mu_w)^{0.14}$	developed for circular tube, Re > 10000
5	Dittus-Boelter [20]	$\mathrm{Nu}_D = 0.0243\,\mathrm{Re}_D^{4/5}\,\mathrm{Pr}^{0.4}$ for heating $\mathrm{Nu}_D = 0.0265\,\mathrm{Re}_D^{4/5}\,\mathrm{Pr}^{0.3}$ for cooling	developed for circular tube, Re > 10000
6	Gnielinski [21]	$\mathrm{Nu}_D = \frac{(f/8)(\mathrm{Re}_D - 1000)\,\mathrm{Pr}}{1 + 12.7(f/8)^{1/2}(\mathrm{Pr}^{2/3} - 1)}$ friction factor according to Moody´s diagram smoth pipes $f = (1.82\log_{10}\mathrm{Re}_D - 1.64)^{-2}$	developed for circular tube, more accurate, 3000 < Re < 5 x 10^6
7	Petukhov [22]	$\mathrm{Nu}_D = \frac{(f/8)\,\mathrm{Re}_D\,\mathrm{Pr}}{1 + 12.7(f/8)^{1/2}(\mathrm{Pr}^{2/3} - 1)}$ friction factor according to Moody´s diagram smoth pipes $f = (1.82\log_{10}\mathrm{Re}_D - 1.64)^{-2}$	circular tube, more accurate, 3000 < Re < 5 x 10^6

6.6.1. Transition flow region (2300 < Re < 6000)

Hausen [23] presented the following empirical correlation for the average Nusselt number beginning of the heated section and the position L for flow in a tube:

$$\mathrm{Nu}_D = 0.116\left(\mathrm{Re}_D^{2/3} - 125\right)\mathrm{Pr}^{1/3}\left[1 + \left(D_h/L\right)^{2/3}\right]\left(\mu/\mu_w\right)^{0.14} \qquad [-] \qquad (15)$$

6.6.2. Laminar flow region (Re < 2300)

For laminar flow, the use of circular tube correlations is less accurate, particularly for cross sections characterized by sharp corners. For such cases the Nusselt number corresponding to fully developed conditions may be obtained from the following empirical correlation developed for laminar flow between two parallel flat plates with one side insulated and the other subjected to a constant heat flux [24]:

$$\mathrm{Nu}_D = 5.4 + \frac{0.0019\left[\mathrm{Re}\,\mathrm{Pr}\left(D_h/L\right)\right]^{1.71}}{1 + 0.00563\left[\mathrm{Re}\,\mathrm{Pr}\left(D_h/L\right)\right]^{1.17}} \qquad [-] \qquad (16)$$

6.7. Radiation heat exchange between frame and adjacent ambient surfaces

Radiation heat transfer coefficient between exterior surface of collector back frame and adjacent surfaces in ambient environment (roof) related to ambient temperature ϑ_{amb} can be expressed as

$$h_{r,b2-amb} = \frac{\sigma}{\frac{1}{\varepsilon_{b2}} + \frac{1}{\varepsilon_{as}} - 1}\frac{\vartheta_{b2}^4 - \vartheta_{amb}^4}{\vartheta_{b2} - \vartheta_{amb}} \qquad [\mathrm{W/m^2.K}] \qquad (17)$$

6.2. Reverse temperature calculation

6.2.1. Mode 1

In steady state, the performance of a solar collector is described by an energy balance that indicates the distribution of incident solar energy into useful energy gain, thermal losses, and optical losses. The solar radiation absorbed by a collector per unit area of absorber A_{abs} is equal to the difference between the incident solar radiation and the optical. The thermal energy lost from the collector to the surroundings by conduction, convection, and infrared radiation can be represented as the product of heat transfer coefficient U, times the difference between the mean fluid temperature ϑ_{fluid} and the ambient temperature ϑ_{amb}:

$$\dot{Q}_u = A_{abs}F'\left[\tau_n\alpha_{abs}G_t - U\left(\vartheta_{fluid} - \vartheta_{amb}\right)\right] \qquad [\mathrm{W}] \qquad (18)$$

The problem with this equation is that the overall heat loss coefficient U and the collector efficiency factor F' is difficult to calculate. The algebra is somewhat tedious and only results of deriving F' and U are presented in Fig. 5. More information about F' and U deriving can be found in Duffie and Beckman [25].

Design 1

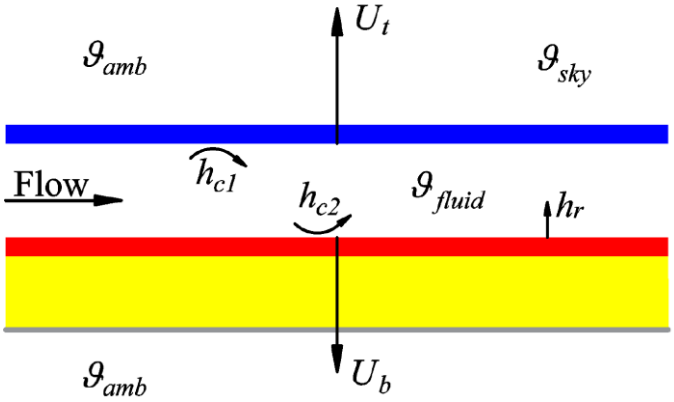

$$U = \frac{(U_b + U_t)(h_{c1}h_{c2} + h_{r,abs-f2}h_{c1} + h_{r,abs-f2}h_{c2}) + U_b U_t (h_{c1} + h_{c2})}{h_{c1}h_{r,abs-f2} + h_{c2}U_t + h_{c2}h_{r,abs-f2} + h_{c1}h_{c2}} \quad [\mathrm{W/m^2.K}] \qquad (19)$$

$$F' = \frac{h_{r,abs-f2}h_{c1} + h_{c2}U_t + h_{c2}h_{r,abs-f2} + h_{c1}h_{c2}}{(U_t + h_{r,abs-f2} + h_{c1})(U_b + h_{c2} + h_{r,abs-f2}) - h_{r,abs-f2}^2} \quad [-] \qquad (20)$$

Design 2

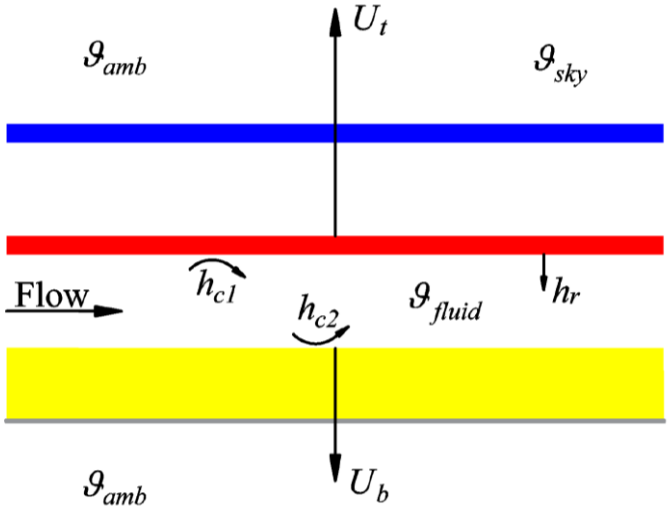

$$U = U_t + U_b \quad [\mathrm{W/m^2.K}] \qquad (21)$$

$$F' = \frac{1}{1 + \dfrac{U}{h_{c1} + \dfrac{1}{\dfrac{1}{h_{c2}} + \dfrac{1}{h_{r,abs-b2}}}}} \quad [-] \qquad (22)$$

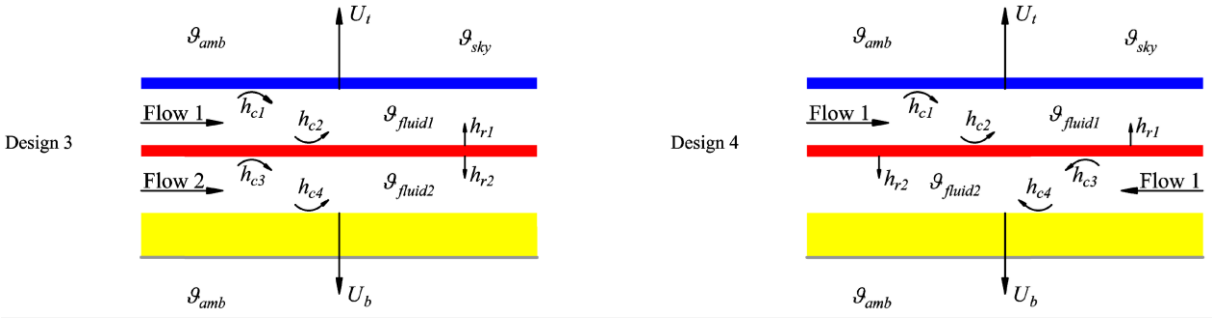

Fig. 5 – Overall heat loss coefficients and efficiency factors for different solar air collector designs (Design 3 and 4 not available yet)

After that the collector flow factor F'' and the collector heat removal factor F_R can be obtained as follows

$$F'' = \frac{\dot{m}c_f}{A_{abs}UF'}\left[1-\exp\left(-\frac{A_{abs}U}{\dot{m}c_f F'}\right)\right] \quad [-] \tag{23}$$

where

c_f is specific thermal capacity of fluid, J/kg.K;

$\dot{m}$ total mass flow rate of fluid through air channel, kg/s,

$$F_R = F''F' \quad [-] \tag{24}$$

Then the useful energy gain is determined

$$\dot{Q}_u = A_{abs}F_R\left[\tau_n\alpha_{abs}G_t - U\left(\vartheta_{in}-\vartheta_{amb}\right)\right] \quad [W] \tag{25}$$

and the outlet temperature

$$\vartheta_{out} = \vartheta_{in} + \frac{\dot{Q}_u}{\dot{m}c_f} \quad [K] \tag{26}$$

Since the useful heat energy gain, the collector heat removal factor and the collector efficiency factor have been calculated for first estimates of temperatures, next iteration step should follow. To calculate heat transfer coefficients at main surfaces of solar collector and to assess the overall collector heat loss coefficient U in the next iteration step the absorber temperature, the mean fluid temperature, and the temperature distribution should be derived

$$\vartheta_{abs} = \vartheta_{in} + \frac{\dot{Q}_u}{F_R U A_{abs}}\left(1-F_R\right) \quad [K] \tag{27}$$

$$\vartheta_{fluid} = \vartheta_{in} + \frac{\dot{Q}_u}{F_R U A_{abs}}\left(1-F'''\right) \quad [K] \tag{28}$$

$$\vartheta_{f2} = \frac{\vartheta_{abs}\left(h_{r,abs-f2}+h_{nc}\right)-U_t\left(\vartheta_{abs}-\vartheta_{amb}\right)}{h_{r,abs-f2}+h_{nc}} \quad [K] \tag{29}$$

$$\vartheta_{f1} = \frac{\vartheta_{f2} h_{cd,f1-f2} - U_t\left(\vartheta_{abs} - \vartheta_{amb}\right)}{h_{cd,f1-f2}} \quad [\mathrm{K}] \tag{30}$$

$$\vartheta_{b2} = \frac{\vartheta_{fluid} h_{c2} + \vartheta_{abs} h_{r,abs-b2} + U_b \vartheta_{amb}}{h_{c2} + h_{r,abs-b2} + U_b} \quad [\mathrm{K}] \tag{31}$$

$$\vartheta_{b1} = \frac{\vartheta_{b2} h_{cd,b1-b2} - U_b\left(\vartheta_{b2} - \vartheta_{amb}\right)}{h_{cd,b1-b2}} \quad [\mathrm{K}] \tag{32}$$

6.2 Mode 2

Mode 2 operates in a principally different manner. The core of the Mode 2 is a set of heat balance equations obtained from the thermal network at the points:

$$\vartheta_{f1}: \quad h_{r,f1-amb}\left(\vartheta_{f1} - \vartheta_{sky}\right) + h_{w,f1-amb}\left(\vartheta_{f1} - \vartheta_{amb}\right) = h_{cd,f1-f2}\left(\vartheta_{f2} - \vartheta_{f1}\right) \tag{33}$$

$$\vartheta_{f2}: \quad h_{cd,f1-f2}\left(\vartheta_{f2} - \vartheta_{f1}\right) = h_{r,abs-f2}\left(\vartheta_{abs} - \vartheta_{f2}\right) + h_{nc}\left(\vartheta_{abs} - \vartheta_{f2}\right) \tag{34}$$

$$\vartheta_{abs}: \quad \tau\alpha G K_{net} = \left(h_{r,abs-f2} + h_{nc}\right)\left(\vartheta_{abs} - \vartheta_{f2}\right) + h_{r,abs-b2}\left(\vartheta_{abs} - \vartheta_{b2}\right) + h_{c1}\left(\vartheta_{abs} - \vartheta_{fluid}\right) \tag{35}$$

$$\vartheta_{fluid}: \quad h_{c1}\left(\vartheta_{abs} - \vartheta_{fluid}\right) = h_{c2}\left(\vartheta_{fluid} - \vartheta_{b2}\right) + \frac{2mc_f}{ac}\left(\vartheta_{fluid} - \vartheta_{in}\right) \tag{36}$$

$$\vartheta_{b2}: \quad h_{r,abs-b2}\left(\vartheta_{abs} - \vartheta_{b2}\right) + h_{c2}\left(\vartheta_{fluid} - \vartheta_{b2}\right) = h_{cd,b1-b2}\left(\vartheta_{b2} - \vartheta_{b1}\right) \tag{37}$$

$$\vartheta_{b1}: \quad h_{cd,b1-b2}\left(\vartheta_{b2} - \vartheta_{b1}\right) = h_{r,b2-amb}\left(\vartheta_{b2} - \vartheta_{amb}\right) + h_{w,b1-amb}\left(\vartheta_{b2} - \vartheta_{amb}\right) \tag{38}$$

By rearranging, we obtain a system of linear equations in the matrix form:

$$\begin{bmatrix} h_{r,f1-amb} + h_{w,f1-amb} + h_{cd,f1-f2} & -h_{cd,f1-f2} & 0 & 0 \\ -h_{cd,f1-f2} & h_{cd,f1-f2} + h_{r,abs-f2} + h_{nc} & -h_{r,abs-f2} - h_{nc} & 0 \\ 0 & -h_{r,abs-f2} - h_{nc} & h_{r,abs-f2} + h_{nc} + h_{r,abs-b2} + h_{c1} & -h_{c1} \\ 0 & 0 & h_{c1} & -h_{c1} - h_{c2} - \frac{2mc_f}{ac} \\ 0 & 0 & h_{r,abs-b2} & h_{c2} \\ 0 & 0 & 0 & 0 \end{bmatrix} \tag{39}$$

$$\begin{bmatrix} 0 & 0 \\ 0 & 0 \\ -h_{r,abs-b2} & 0 \\ h_{c2} & 0 \\ -h_{r,abs-b2} - h_{c2} - h_{cd,b1-b2} & h_{cd,b1-b2} \\ h_{cd,b1-b2} & h_{r,b1-amb} + h_{w,b1-amb} + h_{cd,b1-b2} \end{bmatrix} \begin{bmatrix} \vartheta_{f1} \\ \vartheta_{f2} \\ \vartheta_{abs} \\ \vartheta_{fluid} \\ \vartheta_{b2} \\ \vartheta_{b1} \end{bmatrix} = \begin{bmatrix} h_{r,f1-amb}\vartheta_{sky} + h_{w,f1-amb}\vartheta_{amb} \\ 0 \\ \tau\alpha G K_{net} \\ \frac{2mc_f}{ac}\vartheta_{in} \\ 0 \\ h_{r,b1-amb}\vartheta_{amb} + h_{w,b1-amb}\vartheta_{amb} \end{bmatrix}$$

In general, the above matrices may be displayed as

$$[A][T] = [B] \tag{40}$$

The mean temperature vector may be determined by matrix inversion as

$$[T]=[A]^{-1}[B] \tag{41}$$

Then the outlet fluid temperature and the useful energy gain can be determined

$$\vartheta_{out}=2\vartheta_{fluid}-\vartheta_{in} \qquad [\mathrm{K}] \tag{42}$$

$$\dot{Q}_u=mc_f\left(\vartheta_{fluid}-\vartheta_{in}\right) \qquad [\mathrm{W}] \tag{43}$$

6.3. Iterative procedure

The newly-calculated temperatures values ϑ_{out}, ϑ_{abs}, and ϑ_{fluid} are then compared with previously assumed ones. The iterative process is repeated until all consecutive outlet temperatures, absorber temperatures, and heat transfer fluid temperatures differ by less than 0.01 K. Normally, the number of iterations required is not more than four or five.

6.4. Instantaneous efficiency

Finally, the instantaneous solar air collector efficiency is

$$\eta=\frac{\dot{Q}_u}{A_G G_t} \qquad [-] \tag{44}$$

where

G_t is total radiation for collector surface, W/m^2;

$$G_t=\left(G_{beam}+G_{sky}+G_{gnd}\right)K_{net} \qquad [\mathrm{W/m^2}] \tag{45}$$

where

K_{net} is net incident angle modifier.

6.5. Incident angle modifier K_{net}

The collector absorbs only a portion of the solar irradiance due to the optical properties of the transparent cover and absorber plate, which are described in the $\tau_n\alpha_{abs}$ and the *IAM* parameters for each irradiance component (K_{beam}, K_{sky}, K_{gnd}). Incident angle modifiers are calculated separately for beam (G_{beam}), sky (G_{sky}) and ground radiation (G_{gnd}). The net incident angle modifier for all incident radiation is calculated by weighting each component by the corresponding modifier.

$$K_{net}=\frac{G_{beam}K_{beam}+G_{sky}K_{sky}+G_{gnd}K_{gnd}}{G_t} \qquad [-] \tag{46}$$

Incidence angle modifier of solar collector for beam radiation component can be determined by experiment:

$$K_{beam}=1-b_0\left(\frac{1}{\cos\theta}-1\right)-b_1\left(\frac{1}{\cos\theta}-1\right)^2 \qquad [-] \tag{47}$$

Sky and ground reflected radiation are considered as diffuse isotropic, that means optical properties for this solar radiation components are not considered as incidence angle dependent like for beam radiation but constant. Incidence angle modifier of solar collector for sky and ground radiation components can be approximated using Brandemuehl and Beckman's equations [29] from the K_{beam} characteristic for given effective incident angle:

$$\theta_{eff,sky} = 59.68 - 0.1388\varphi + 0.001497\varphi^2 \quad [°] \quad (48)$$

$$\theta_{eff,gnd} = 90 - 0.5788\varphi + 0.002693\varphi^2 \quad [°] \quad (49)$$

Finally incident angle modifiers for sky-diffuse and ground-reflected radiation are:

$$K_{sky} = 1 - b_0\left(\frac{1}{\cos\theta_{eff,sky}} - 1\right) - b_1\left(\frac{1}{\cos\theta_{eff,sky}} - 1\right)^2 \quad [-] \quad (50)$$

$$K_{gnd} = 1 - b_0\left(\frac{1}{\cos\theta_{eff,gnd}} - 1\right) - b_1\left(\frac{1}{\cos\theta_{eff,gnd}} - 1\right)^2 \quad [-] \quad (51)$$

In the case of $b_1 = 0$, incident angle modifiers for beam, sky and ground radiation have to be calculated by another equations:

$$K_{beam} = 1 - b_0\left(\frac{1}{\max(0.5, \cos\theta)} - 1\right) - \frac{(1-b_0)(\max(60,\theta) - 60)}{30} \quad [-] \quad (52)$$

$$K_{sky} = 1 - b_0\left(\frac{1}{\max(0.5, \cos\theta_{eff,sky})} - 1\right) - \frac{(1-b_0)(\max(60,\theta_{eff,sky}) - 60)}{30} \quad [-] \quad (53)$$

$$K_{gnd} = 1 - b_0\left(\frac{1}{\max(0.5, \cos\theta_{eff,gnd})} - 1\right) - \frac{(1-b_0)(\max(60,\theta_{eff,gnd}) - 60)}{30} \quad [-] \quad (54)$$

7. Experimental validation (to be added in 2018)

8. References

[1] Hottel H, Woertz B. Performance of flat-plate solar-heat collectors. Trans ASME (Am Soc Mech Eng); (United States) 1942;64:91–104.

[2] Hottel H, Whillier A. Evaluation of flat-plate solar collector performance. Trans Conf Use Sol Energy; 1955;3:74–104.

[3] Bliss Jr. RW. The derivations of several "Plate-efficiency factors" useful in the design of flat-plate solar heat collectors. Sol Energy 1959;3:55–64. doi:10.1016/0038-092X(59)90006-4.

[4] Smith CC, Weiss TA. Design application of the Hottel-Whillier-Bliss equation. Sol Energy 1977;19:109–13. doi:10.1016/0038-092X(77)90047-0.

[5] Mcadams WH. Heat Transmission 3d Ed. New York: McGraw-Hill; 1954.

[6] J. H. DW, W. W. S. C, Proctor. Solar and wind induced external coefficients for solar collectors. Coop Mediterr Pour l'Energie Solaire, Rev Int d'Heliotechnique 1977;2:56.

[7] Test FL, Lessmann RC. An Experimental Study of Heat Transfer During Forced Convection over a Rectangular Body. J Heat Transfer 1980;102:146–51.

[8] Test FL, Lessmann RC, Johary A. Heat Transfer During Wind Flow over Rectangular Bodies in the Natural Environment. J Heat Transfer 1981;103:262–7.

[9] Kumar S, Sharma VB, Kandpal TC, Mullick SC. Wind induced heat losses from outer cover of solar collectors. Renew Energy 1997;10:613–6. doi:10.1016/S0960-1481(96)00031-6.

[10] Hollands KGT, Unny TE, Raithby GD, Konicek L. Free Convective Heat Transfer Across Inclined Air Layers. J Heat Transfer 1976;98:189–93.

[11] Buchberg H, Catton I, Edwards DK. Natural Convection in Enclosed Spaces - A Review of Application to Solar Energy Collection. J Heat Transfer 1976;98:182–8.

[12] Randall KR, Mitchell JW, El-Wakil MM. Natural Convection Heat Transfer Characteristics of Flat Plate Enclosures. J Heat Transfer 1979;101:120–5.

[13] Schinkel W. Natural concection in inclined air-filled enclosures. Delft: Dutch Efficiency Bureau - Pijnacker; 1980.

[14] Niemann H. Die Wärmeübertragung durch natürliche Konvektion in spaltförmigen Hohlräumen. Gesund Ing 1948;69:224–8.

[15] Matuska T, Zmrhal V. A mathematical model and design tool KOLEKTOR 2.2 reference handbook. Prague: 2009.

[16] Kays WM, Crawford ME. Convective Heat and Mass Transfer, 2nd edn McGraw-Hill. New York 1980:141.

[17] Tan HM, Charters WWS. Effect of thermal entrance region on turbulent forced-convective heat transfer for an asymmetrically heated rectangular duct with uniform heat flux. Sol Energy 1969;12:513–6. doi:10.1016/0038-092X(69)90072-3.

[18] Nusselt W. Der Wärmeaustausch zwischen Wand und Wasser im Rohr. Forsch Auf Dem Gebiete Des Ingenieurwesens 1931;2:309–13. doi:10.1007/BF02583210.

[19] Sieder EN, Tate GE. Heat Transfer and Pressure Drop of Liquids in Tubes. Ind Eng Chem 1936;28:1429–35. doi:10.1021/ie50324a027.

[20] Dittus FW, Boelter LMK. Heat transfer in automobile radiators of the tubular type. Int Commun Heat Mass Transf 1985;12:3–22.

[21] Gnielinski V. New equations for heat and mass transfer in turbulent pipe and channel flow. Int Chem Eng 1976;16:359–68.

[22] Petukhov BS. Heat transfer and friction in turbulent pipe flow with variable physical properties. Adv Heat Transf 1970;6:503–64.

[23] Hausen H. Darstellung des Warmeuberganges in Rohren durch verallgemeinerte

Potenzbeziehungen. Z VDI Beih Verfahrenstech 1943;4:91–8.

[24] Heaton HS, Reynolds WC, Kays WM. Heat transfer in annular passages. Simultaneous development of velocity and temperature fields in laminar flow. Int J Heat Mass Transf 1964;7:763–81. doi:10.1016/0017-9310(64)90006-7.

[25] Duffie JA, Beckman WA. Solar engineering of thermal processes. John Wiley & Sons; 2013.

Appendix 1: Installation

The Type206 solar air collector model is a TRNSYS 17 drop-in dll component. For a complete set of files one should have:

Type206.dll – the drop-in dll file

Type206.cpp – the C++ source code

Type206.tmf – the Simulation Studio proforma

Type206.bmp – the Simulation Studio proforma icon

For installation:

1. Copy the .dll file to \TRNSYS16\UserLib\ReleaseDLLs\

2. Copy the .tmf and .bmp files to the \Proformas folder, e.g. C:\Trnsys17\Studio\Proformas\Nonstandard\

3. Restart simulation studio if it was running.